Cryogenics

S. Succi

EUROPEAN ORGANIZATION FOR NUCLEAR RESEARCH

CERN-ISR-VA/69-78

LOW PRESSURE CRYOPUMPING OF HYDROGEN

by

C. Benvenuti and R.S. Calder

Paper to be presented at the
Colloque International "Vide et Froid",
Grenoble (France), December 1969

Geneva - 28th November, 1969

CONTENTS

ABSTRACT

For many years cryopumping seemed the ideal clean pumping method for obtaining high pumping speeds down to extremely low pressure. More recently, however, the value of this technique has been seriously questioned due to an unexpected limitation - the inability to pump appreciable quantities of hydrogen at low pressures. This is a particularly serious limitation because hydrogen is usually the dominant residual gas in UHV systems and because, surprisingly, this low pressure limit could not be lowered by further reduction of the condensing surface temperature.

Results from several cryopump systems will be presented. These indicate that this limit - which appeared as an anomalous temperature independence of the hydrogen saturated vapour pressure curve towards very low temperatures - is a phenomenon strongly dependent on the design of the apparatus and the nature of the condensing surface. By suitable design it has been possible to extend the low pressure usefulness of the cryopump and reproduce experimentally the expected hydrogen saturated vapour pressure curve down to about 1×10^{-11} torr. Data on hydrogen adsorption isotherms and saturated vapour pressures within the range 10^{-12} to 10^{-6} torr will be presented.

1. Introduction

The technique of cryopumping with its important potential advantages of extreme cleanliness, high speed and very low ultimate pressure would seem to be the ideal solution for many ultra-high vacuum pumping problems. The only obvious disadvantages are connected with the needs of continuous refrigeration and, sooner or later, of a warm-up of the pump and the removal from the system of the previously cryopumped gas. Excluding helium, which is usually absent from all-metal U.H.V. systems, hydrogen remains as the most difficult gas to cryopump. Unfortunately it is nearly always the dominant component of the gas load in an ultra-high vacuum system[1].

It is to be expected that at a pressure p the speed S of a cryopump would be given by

$$S = \alpha S_o (1 - P/p) \quad \text{or} \quad = \alpha S_o (1 - P'/p)$$

where S_o is the conductance of the pumping surface for the gas being considered with a sticking coefficient α and a saturated vapour pressure of P, or an equilibrium pressure P' determined by the surface coverage if unsaturated. Clearly the ultimate pressure of the pump is P when operating in the condensing or saturated condition. Before saturation occurs the limit pressure P' will be lower, but this mode of operation is, in general, less useful because the value of P' is continuously increasing with the quantity of gas pumped and will finally reach the limit P.

In the saturated condition a cryopump should be able to condense further unlimited quantities of gas without change of speed or limit pressure P - the latter, ideally, being only a function of the gas and the operating temperature. Figure 1 shows the experimental and extrapolated low temperature saturated vapour pressure data for hydrogen from several authors[2,3,4] in the range 10^{-6} to 10^{-9} torr (i.e. 4.2 to 3.3°K). These data are

closely approximated by the simplified form of the Clausius-Clapeyron equation, Log P = A - B/T, where A and B are constants with B = E/R (E, heat of sublimation per mole and R, gas constant per mole). Extrapolation to 2.5°K gives a saturated vapour pressure well below 10^{-12} torr for hydrogen. At this temperature, which is easily achieved using liquid helium, all other gases, excluding helium, have a negligible vapour pressure.

2. Apparatus

The Intersecting Storage Rings now being constructed at CERN will comprise more than 2 km of ultra-high vacuum chamber in which a high energy proton beam will circulate more or less continuously. The bakeable vacuum chamber, constructed from stainless steel, will operate at ~ 10^{-9} torr average pressure. An important additional requirement will be that local regions, a few metres in extent (the experimental intersection regions), must operate at pressures around 10^{-11} torr or better. It has been considered[5] these requirements could be met by placing several cryopumps operating at 2.5°K around such an experimental region.

A cryopump used in the manner outlined here should not only pump the region under question but also act as a trap to impede the flow of gas from the rest of the vacuum chamber at 10^{-9} torr. There must, however, be a straight line-of-sight passage for the proton beam. These considerations led to the preliminary cryopump design in Fig. 2 - the model A pump - in which the proton beam passes through the lower part of the pump. The pump, between the flanges AA', will form an integral part of about 1 m of the ISR vacuum chamber.

The model A cryopump consists essentially of a central stainless steel liquid helium reservoir, the outside of which acts as the condensing surface. The conduction cooled copper radiation shield at ~ 77°K of the design shown reduces the radiant heat imput to an acceptable value while still permitting free circulation of the proton beam. The diameter of this shield

(about 500 mm) and the beam aperture dimensions (a horizontal ellipse of 160 mm x 50 mm) primarily determine the trapping efficiency of the pump. Measurements showed that for hydrogen a pressure ratio of approximately 30 could be maintained between the points A and A'.

The gas injection and analysing equipment shown outside the region AA' were used for evaluating the pumping and trapping characteristics. In later experiments high purity hydrogen could be injected via a palladium leak and bakeable valve. Condensing surface temperatures could be regulated and controlled to $0.001^{\circ}K$ in the range 4.2 to $2.3^{\circ}K$ (or lower) and could be measured to $0.01^{\circ}K$ using the measurement of the helium vapour pressure or using resistance thermometers placed at the bottom of the helium bath. Pressure measuring and analyzing equipment shown in Figs 2 and 3 was calibrated for absolute reading to about ± 10% using a standard gauge[6,7]. This accuracy is expected to be good down to the 10^{-10} torr range, but to deteriorate considerably in the 10^{-11} torr range (± 50%). Due to sensitivity limitations readings in the lower 10^{-12} torr range cannot be taken as more than approximate indications of the pressure. Relative pressures and pressure changes are, of course, considerably more reliable. Thermomolecular corrections, which are discussed in Section 3 and have been applied to all our data, displace these sensitivity limits downwards by one order of magnitude.

The model B cryopump shown in Fig. 3 differs only from the model A in construction of the liquid helium reservoir. Again it is stainless steel but the sides and supporting and pumping tube are constructed with a double wall and an independent evacuated space. This has the result of isolating effects arising from temperature gradients within the liquid helium and from variations of liquid helium level or rate of helium boil-off (and hence cooling power to the upper part of the reservoir) from the main vacuum system. This greatly facilitates the problem of defining and maintaining the pumping surface at a constant and uniform temperature. The area of the low temperature surface

is further defined by a second, close fitting copper screen at $\sim 77^{\circ}K$.

3. Hydrogen saturated vapour pressure data

Figure 4 shows experimental data for the hydrogen saturated vapour pressure as a function of temperature from measurements using the model A and B cryopumps. Over the common temperature interval ($4.2 - 3.3^{\circ}K$) both sets of data are consistent and agree satisfactorily with those from Fig. 1. The slope of the Log P vs 1/T plot, which gives a heat of sublimation of 192 calories per mole, compares reasonably with 184 (Ref. 2), 206 (Ref. 3) and 220 calories per mole (Ref. 4). The agreement in absolute pressure, where calibration is more difficult, is not so close.

Below $3.3^{\circ}K$ our experimental data for the saturated vapour pressure begin to depart systematically from the Clausius-Clapeyron relation $\text{Log } P = A - B/T$, and finally settle at a constant limiting value which is, within the limits of error, temperature independent. This limiting pressure, which obviously restricts the low pressure usefulness of the cryopump, was not, with the model A cryopump, at all reproducible from one experiment to the next. Moreover, it was often extremely unstable but, as indicated, it was usually within the range 3×10^{-11} to 3×10^{-10} torr. The model B cryopump, see Fig. 3, which was designed to overcome these difficulties, behaved much more satisfactorily with completely reproducible results but still gave a temperature independent low pressure limit. The limit was now close to 2×10^{-11} torr. In all cases this limiting hydrogen saturation vapour pressure was significantly higher than the 1 to 3×10^{-12} torr limit of the cryopump observed before injecting hydrogen. This system or gauge limit, marked Po on the figures and which differed slightly from one instrument to the other depending on their degree of contamination, has been substracted from the observed values before plotting. In most cases it has a very small effect. The data are also corrected for

hydrogen sensitivity and thermo-molecular transpiration to give pressure readings appropriate to the temperature being considered. This means that the observed pressures in the warm parts of the apparatus were roughly a factor of ten higher than the values plotted.

A similar departure of the hydrogen saturated vapour pressure from the expected temperature variation has also been reported by Chubb at al.[8]. In these results the limit, using our method of presentation, corresponded to a pressure of about 3×10^{-10} torr. The unexpected nature of this limit and its variation between one apparatus and another has led us to suppose, and hope, that it is more of a phenomenon connected with the design of the cryopump than a fundamental property of condensed hydrogen films. Chubb et al.[8] have proposed an explanation based on an increased rate of desorption induced by thermal radiation originating from warmer parts of the cryopump and adsorbed by the condensed H_2. Experimental measurements were made to support this hypothesis. We have not been able to verify this suggestion and it seems probable that it is not the whole explanation. In addition to finding a similar limit at 2×10^{-10} torr with a small experimental cryosurface, which was completely exposed to ambient temperature surfaces and which received about 45 m.Watt cm^{-2} and adsorbed about 4 m.Watt cm^{-2} we found, using the model B cryopump (where the radiation is estimated at about 1 m.Watt incident and 0.1 m.Watt adsorbed), a complex behaviour of this limit pressure. It appears to depend on the quantity of hydrogen condensed, the purity of the injected hydrogen and, possibly, the nature of the condensing surface. It would seem probable that all these factors could be operating to give anomalously high limit pressure at the lowest temperatures and moreover, with our apparatus, we cannot exclude without further experimentation additional possibilities such as the continuous transport of energy to the condensed hydrogen by molecules that evaporate at about $3^{\circ}K$ and return at about $77^{\circ}K$.

Only measurements made in a completely isothermal enclosure can entirely eliminate all possible sources of error - but such a system presents serious difficulties to the measurement of very low pressures.

4. Factors influencing the low pressure limit

In this section we turn to a detailed study of the adsorption and condensation of hydrogen on stainless steel. In a following section some preliminary results using condensed argon as the substrate will be presented. All measurements were made on the model B cryopump, which has proved to be useful and fairly versatile for these measurements in spite being designed as a practical and rather special cryopump.

Figure 5 shows the influence of the quantity of condensed hydrogen on the saturated vapour pressure curve. Results were reproducible over several experiments using arbitrarily chosen surface concentrations of 2×10^{16} molecules cm^{-2} (about twice the quantity needed for saturation) and 22×10^{16} molecules cm^{-2}. The data for 2×10^{16} molecules cm^{-2} are, in part, the same as presented and discussed in Fig. 4 for the model B cryopump. The differences introduced by condensing a thicker layer of hydrogen may be summarised as

a) a considerably lower limit pressure on both the total pressure gauge and the mass analyser - in fact, the H_2 peak on the latter decreased continuously into the noise level without showing a significant departure from the extrapolated saturated vapour pressure curve,

b) a strong disagreement of total pressure reading and H_2 peak although no other peaks could be found on the mass analyser,

c) a much slower approach to equilibrium of about 15 hours after injection of 22×10^{16} molecules cm^{-2} of hydrogen at $2.3^{\circ}K$, compared with 2 hours for 2×10^{16} molecules cm^{-2}.

The hydrogen used in all experiments until this point was, as judged by the mass analyser on the injection side of the pump, about 99% H_2 and 1% N_2, with all other components very much smaller. At this point we introduced into the injection system a palladium leak purifier which gave $H_2 > 99.9\%$ and $N_2 < 0.1\%$. Figure 6 shows, as a function of time, the approach to equilibrium after injecting various quantities of hydrogen of both 99% and 99.9% purity. In all cases the pressure during injection was maintained close to 1×10^{-9} torr and the condensing surface held at $2.3^{\circ}K$. The use of higher purity hydrogen at once restores the agreement between gauge and mass analyser for large injections and reduced considerably the times necessary to achieve equilibrium. In addition, however, the use of the higher purity hydrogen raises the low pressure limit attainable, giving a limit still dependent on the quantity of H_2 and independent of the temperature.

We cannot be entirely sure which of these effects are related to the condensed hydrogen film and which are artefacts from the measuring instruments. The dependence of agreement between gauge reading and mass analyser (a Leybold type omegatron) on the hydrogen purity could well be a result of contamination during the injection period of up to one hour at 1×10^{-9} torr; similarly the variable rate of approach to equilibrium could be an instrumental phenomenon or contamination. But the dependence of the limit pressure on the quantity of pure H_2 (a lower limit after a larger injection) and lower H_2 peak using less pure material would seem to be phenomena related to the condensed film. Figure 7 shows the adsorption isostere for a saturated film (66×10^{16} molecules cm^{-2}) of 99.9% pure hydrogen on stainless steel. It represents the closest approach to 'ideal' conditions which we have achieved with our cryostat and, while giving results in the high temperature region identical to those discussed earlier, it still shows a temperature independent low pressure limit of $\sim 8 \times 10^{-12}$ torr.

We have not, in contrast to Chubb et al.[8], found any dependence of the limit pressure on the rate of deposition, which has been varied between the limits of 7×10^{13} to 7×10^{10} molecules cm^{-2} sec^{-1}.

5. Adsorption isotherms for 99.9% pure hydrogen on stainless steel

In this section we consider the form of the experimental adsorption isotherms and isosteres concentrating, in particular, on the unsaturated and just saturated region, i.e. up to about 10^{16} molecules cm^{-2}. Figures 8 and 9 summarise these data, Fig. 8 has been synthesised partly from directly measured isotherms and partly from the isosteric data of Fig. 9. On Fig. 8 three major regions, A, B (subdivided into B_1 and B_2) and C can be distinguished, and these delineate the different isosteric patterns found in Fig. 9.

The region A, which extends up to 0.35×10^{16} molecules cm^{-2}, is the simplest but yet the most puzzling. It shows a pressure increasing with quantity condensed, which is closely approximated by the law $P \propto Q^{1.85}$, but which is, see curve e on Fig. 9, practically temperature independent with heat of sublimation of less than 3 calories per mole.

The region C of Fig. 8, extending above 1.0×10^{16} molecules cm^{-2} and which was discussed more fully in Sections 3 and 4, shows the behaviour of the saturated surface. Here the behaviour is what we would expect except for the limiting low pressure value at low temperatures and the slight dependence of this limit on the film thickness. This behaviour is shown in curves d, f and g of Fig. 9.

The most complex region, and experimentally the most difficult is that marked B_1 and B_2 in Fig. 8 covering the range 0.35×10^{16} to 1.0×10^{16} molecules cm^{-2}. All isotherms exhibit a more or less abrupt kink at 0.35×10^{16} molecules cm^{-2} and 3×10^{-11} torr. Those for temperatures below about $2.8^{\circ}K$ pass a

maximum at this point and fall slightly before levelling out at the saturation value. Those for temperatures above 2.8°K give, for increasing surface concentration, an increasing and then finally a constant saturation pressure. The coverage at which saturation occurs is apparently a function of the temperature, being lower for lower temperatures, and lies in the region B_2, i.e. between 0.5×10^{16} and 1.0×10^{16} molecules cm^{-2}.

The times necessary to achieve equilibrium after making an injection vary considerably from one region to another. In regions A and C it is always relatively short and less than two hours, being temperature independent in A, and varying between two hours for 2.3 - 2.9°K to less than one minute at 4.2°K in C. In the region B the equilibrium time is about two hours for temperatures below 2.9°K, but increases for higher temperatures to reach more than ten hours for 4.2°K and for pressures less than 10^{-8} torr. At higher pressures the behaviour approaches that for region C.

Again all data, as for the saturated vapour pressures showed no dependence on deposition rate.

The adsorption isosteres of Fig. 9 show interesting differences of form and dynamic behaviour in the region B_1 and B_2. On raising the temperature from 2.3 to 4.2°K for an isostere in the region B_1 (e.g. curve c, Fig. 9) there is an initial temperature independence up to 2.9°K. Above this, for each small temperature increase, there is a rapid and relatively large rise of pressure which decays slowly to a much lower equilibrium value over a period of about ten hours. The overall equilibrium result is a small but definite pressure difference, as in curve c, between 2.3 and 4.2°K. Isosteres such as a and b in Fig. 9, within the region B_2, start from the points on the flat (saturated) 2.3°K isotherm, and show an initial behaviour very similar to those of the fully saturated region C. On raising the temperature they are all at first practically temperature independent and then temperature dependent with a slope which increases with condensed quantity and which approaches the full

value of 192 calories per mole. This behaviour, as for the fully saturated isosteres in region C, is without any transient pressure bumps. At a still higher temperature the normal pressure increase is followed by slow decay (the vertical dotted lines of Fig. 9), taking more than ten hours to reach equilibrium. Further temperature increases cause a rise of pressure as shown, but with transient effects as found in the region B_1. A temperature reduction now results in return curves with an initial slope close to 192 calories $mole^{-1}$ and which show considerable hysteresis - at first, lower and then higher (i.e. the curves a' and b', Fig. 9) than the rising curve. This is the origin of the double dotted curves in region B_2 of Fig. 8.

It is tempting to speculate that the temperature independent region A represents the build-up of the first molecular layer with an anomalous vapour pressure which, perhaps, depends on the nature of the substrate and which influences the limiting low pressure value for fully saturated films. Similarly, we may speculate that in the region B the build-up of a second layer starts. Raising the temperature we reach a critical value quantity dependent (the dotted vertical lines, curves a and b, Fig. 9), at which re-organisation of the hydrogen takes place. Alternatively we could think that we are in the presence of two different adsorption states of hydrogen with a temperature dependent probability of transition from one to the other.

6. The adsorption of hydrogen on solid argon

A few preliminary experiments have been made using the model B cryopump and adsorbing hydrogen onto a previously condensed film of argon. Results from two experiments are shown in Fig. 10.

In the first experiment 2.0×10^{16} H_2 molecules cm^{-2} were adsorbed at 2.3°K onto a layer of 3.4×10^{16} molecules cm^{-2} of previously condensed argon. Injection of hydrogen lasted 50 minutes, during which periodic interruptions of the injection

produced a rapid fall over all the range of surface concentrations to the equilibrium base pressure in the low 10^{-12} torr range. The whole injection resulted in a barely detectable increase in equilibrium base pressure, after thermomolecular correction, of not more than 3×10^{-13} torr. After this injection the temperature was raised in steps to $4.2^{o}K$. Initially there was no pressure dependence on temperature - but this is attributed to lack of measuring sensitivity, rather than a limiting pressure as encountered using a stainless steel substrate. Figure 10 shows that from $2.6^{o}K$, the first point above the noise level, the pressure increases regularly from 6.2×10^{-13} torr with absolute values and a temperature dependence exactly as extrapolated from data found previously at higher temperatures using the stainless steel substrate.

In another experiment hydrogen was adsorbed at $4.2^{o}K$ onto a previously condensed argon film of 4.2×10^{16} molecules cm^{-2}. In this example the equilibrium base pressure increased continuously with condensed quantity and, after giving an adsorption isotherm rather similar to that for $4.2^{o}K$ in Fig. 8, reached a constant saturation pressure (of the normal value) at 2.2×10^{16} molecules cm^{-2}. During the measurement of this isotherm the injection was occasionally interrupted and small temperature excursions introduced. Figure 10 shows that, in distinction from the case of adsorption on stainless steel, there is always a temperature dependence with a more or less constant heat of sublimation which is equal to that for the saturated hydrogen film.

7. Conclusion

Although the rather complicated and unexpected behaviour encountered during the cryopumping of hydrogen on stainless steel has not been satisfactorily explained, it is possible, from the present work, to indicate the possible sources of the anomalies. The overall picture emerges of an anomalous first layer which is followed by one, or perhaps two, additional layers exhibiting

temperature dependent re-arrangement or phase-transition phenomena. Still more hydrogen gives the expected saturated vapour pressure at high temperatures but, when condensed on stainless steel, gives a quantity and purity dependent but temperature independent low pressure limit. All anomalies, within the limits of our measurements, appear to be removed by using a condensed argon film as substrate. This substrate gives a heat of sublimation and absolute saturated vapour pressure for adsorbed hydrogen identical for that obtained from a saturated film condensed on stainless steel.

The constancy of saturated hydrogen vapour pressure throughout all our experiments in the range 10^{-6} to about 10^{-10} torr suggests that it could be usefully employed for the calibration of vacuum gauges.

It would appear feasible, now, to cryopump continuously large quantities of hydrogen in the low 10^{-11} torr range although, it must be admitted, the presence of considerable quantities of argon would often be a serious disadvantage.

Further experimentation is needed, especially in the direction to investigate the effects of various substrates and of the surrounding temperature. It appears that the latter, if important, and which may produce an effect by radiation or molecular thermal transport, must be strongly influenced by the nature of substrate. The search for another substrate with properties similar to argon but more ameniable to ultra-high vacuum use must be our next objective.

Acknowledgements

It is a pleasure to acknowledge the continual interest and encouragement in this work from Dr. E. Fischer and to thank Dr. G. Lewin for stimulating and helpful criticism. Also to thank all members of the ISR Vacuum Group for fruitful discussions and, particularly, Messrs. F. Le Normand, L. Derivaz and I. McGregor for invaluable assistance.

References

1) R.S. Calder and G. Lewin

Reduction of stainless steel outgassing in ultra-high vacuum, Brit.J.Appl.Phys. 1967, vol. 13, p. 1459.

2) W. Bächler, G. Klipping and W. Mascher

Cryogenic pump systems down to 2.5°K, Trans. 1962 A.V.S. 9th Vacuum Symposium, Macmillan, p. 216.

3) E.S. Borovik, S.F. Grishin and E. Ya. Grishina

The vapour pressure of nitrogen and hydrogen at low pressures, Soviet Phys. Tech. Phys. 5, 1960, p. 506.

4) R.E. Honig and H.O. Hooke

Vapour pressure data for some common gases, RCA Review, Sept. 1960, p. 360.

5) R.S. Calder and E. Fischer

Vacuum problems related to colliding beam experiments with the CERN Intersecting Storage Rings, CERN report AR/Int. SG/65-18.

6) Chr. Von Meinker and G. Reich

An ionisation gauge of constant sensitivity, Proc. Second European Vacuum Symposium, Frankfurt am Main 1963, p. 233.

7) B. Angerth

Private communication, 1969.

8) J.N. Chubb, L. Gowland and I.E. Pollard

Conclusions from experimental studies of condensation pumping of hydrogen and deuterium on liquid helium cooled surfaces, 5th Symposium on Fusion Technology, Oxford, July 1968.

Figure captions

Fig. 1 : Saturated vapour pressure data for hydrogen

Fig. 2 : Model A cryopump

Fig. 3 : Model B cryopump

Fig. 4 : Saturated vapour pressure data for hydrogen ($\sim$ 99% H_2, $\sim$ 1% N_2) from Model A and Model B cryopumps

Fig. 5 : The influence of the quantity condensed on the saturated vapour pressure behaviour for hydrogen ($\sim$ 99% H_2, $\sim$ 1% N_2) in the Model B cryopump

Fig. 6 : The influence of the hydrogen purity on the equilibrium times and pressures

Fig. 7 : Saturated vapour pressure data for high purity hydrogen ($>$ 99.9%) on stainless steel

Fig. 8 : Adsorption isotherms for hydrogen of high purity ($>$ 99.9%) on stainless steel

Fig. 9 : Adsorption isosteres for hydrogen of high purity ($>$ 99.9%) on stainless steel

Fig. 10 : Isosteres for hydrogen adsorbed on pre-condensed argon films.

FIG 1: SATURATED VAPOUR PRESSURE DATA FOR HYDROGEN

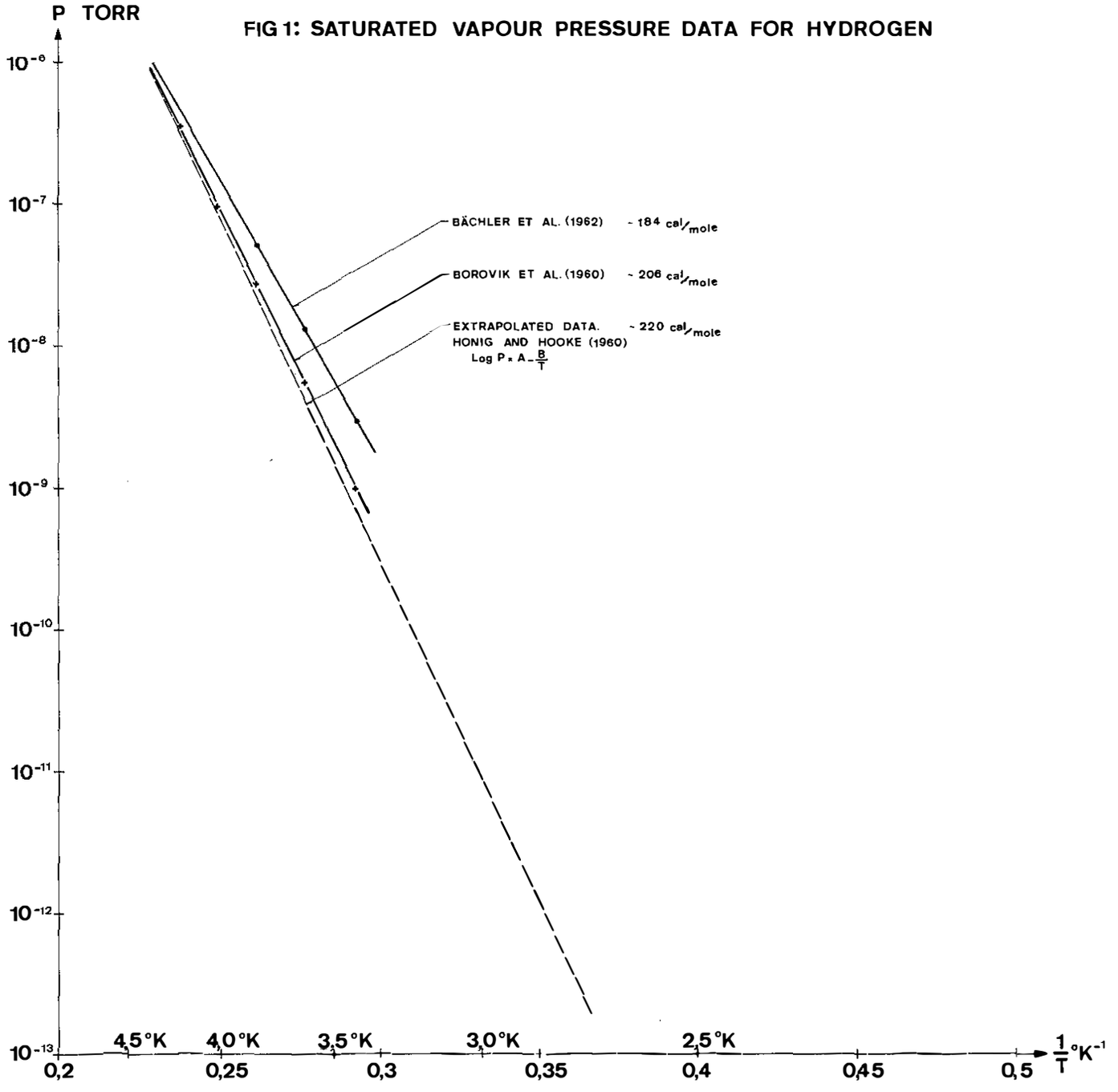

Fig. 2
Model A Cryopump

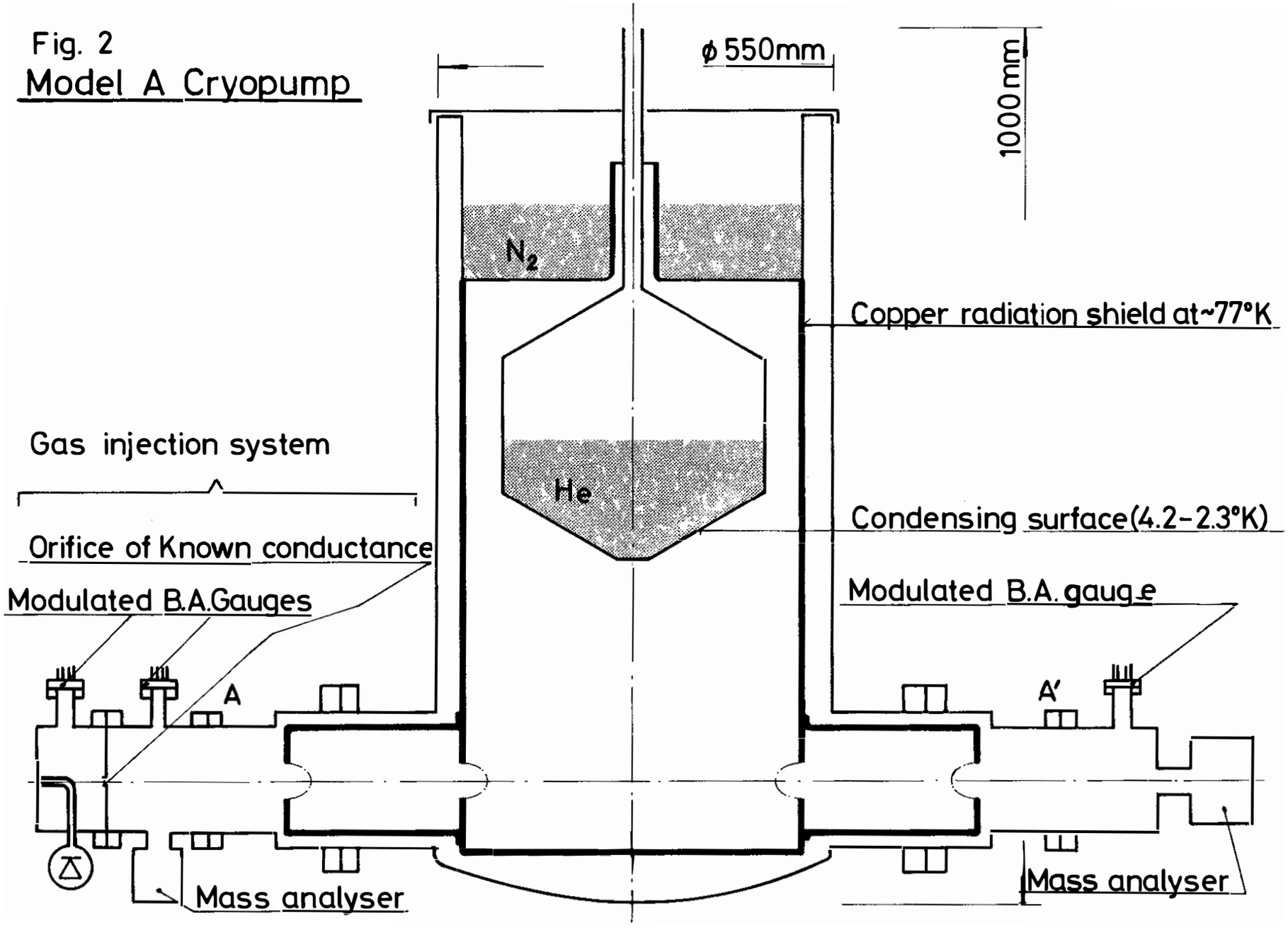

Fig. 3
Model B Cryopump

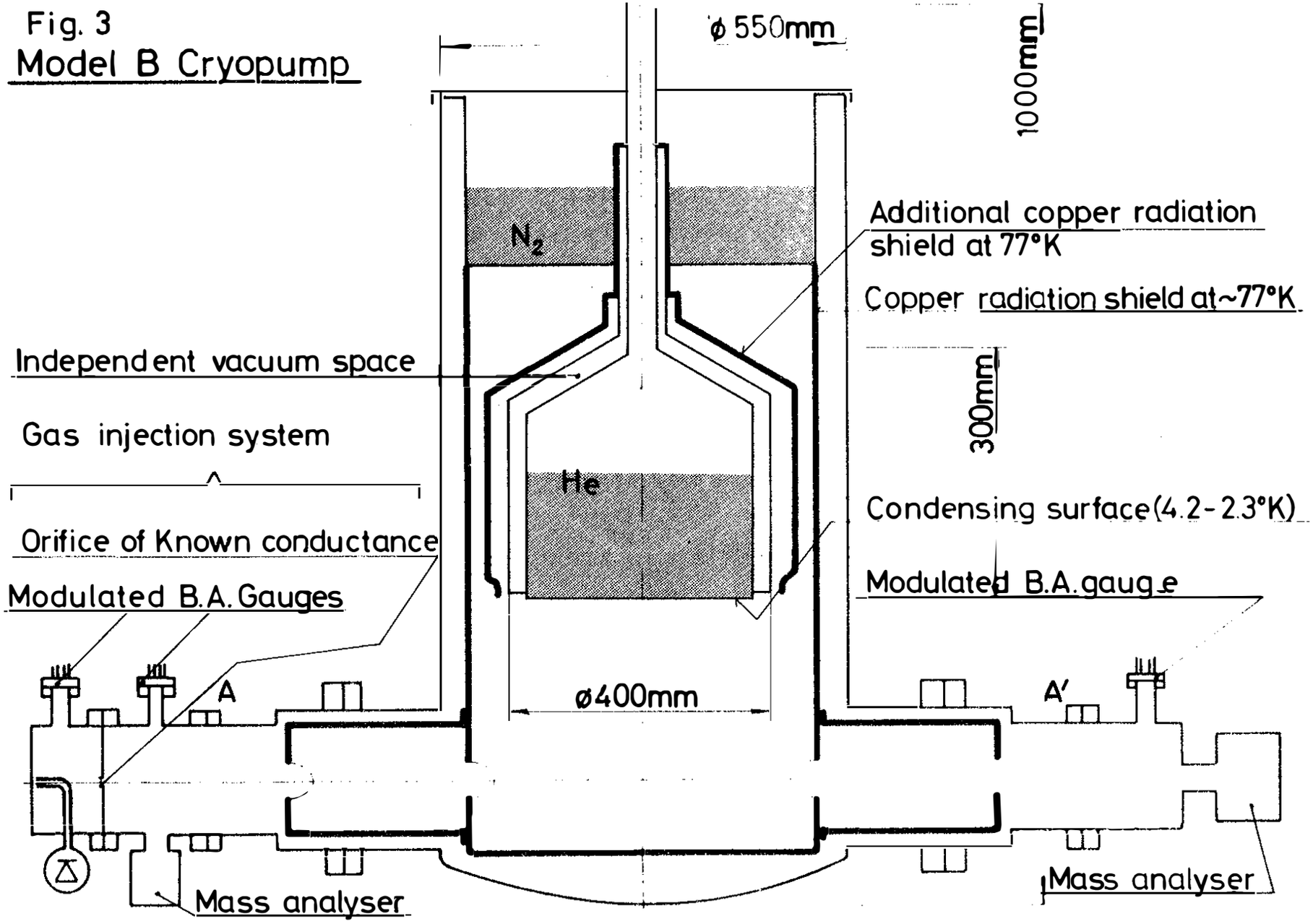

FIG 4 : SATURATED VAPOUR PRESSURE DATA FOR HYDROGEN (~99%H_2,~1%N_2) FROM MODEL A AND MODEL B CRYOPUMPS

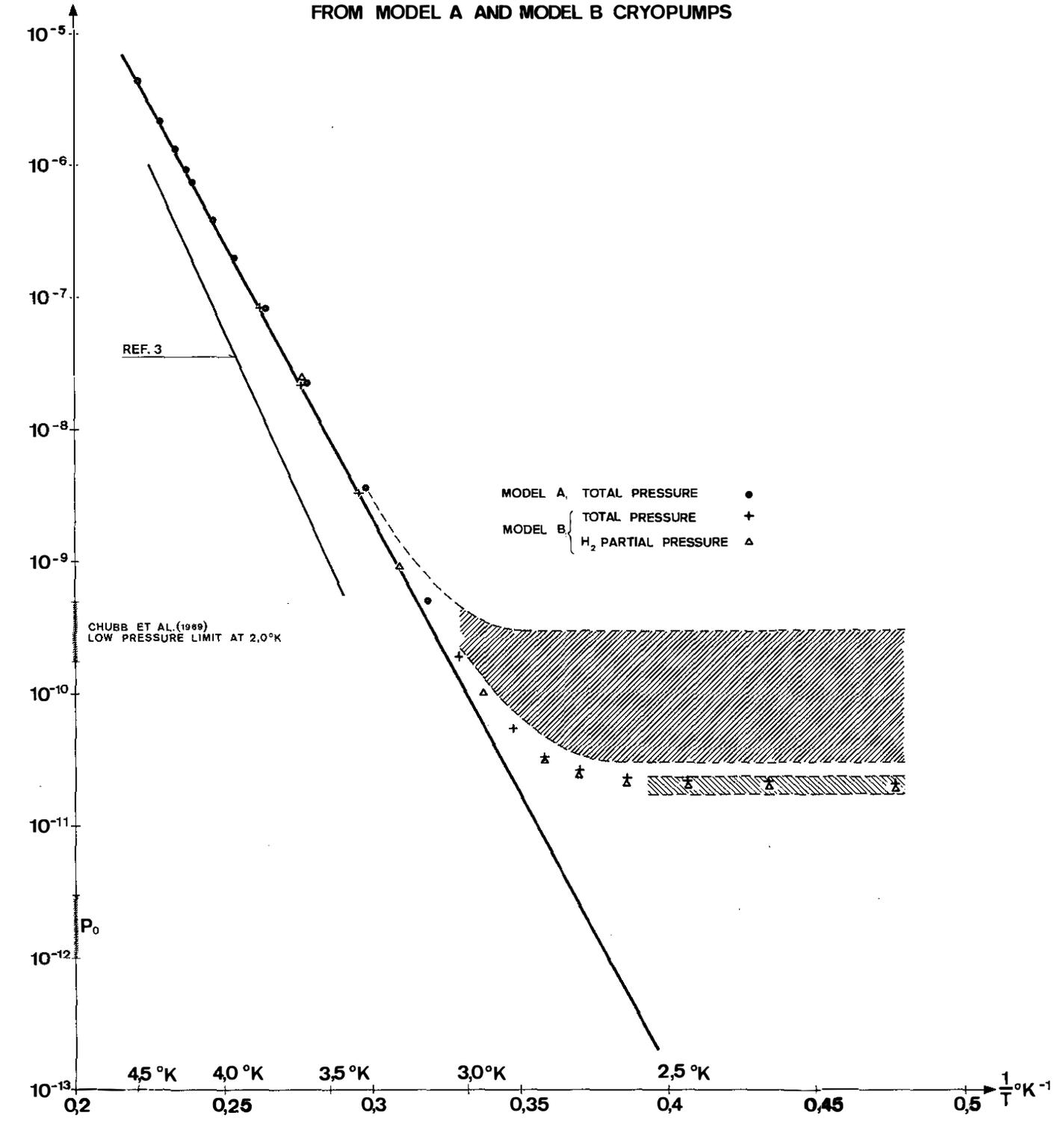

FIG 5: THE INFLUENCE OF THE QUANTITY CONDENSED ON THE SATURATED VAPOUR PRESSURE BEHAVIOUR FOR HYDROGEN (~99 % H_2, ~1 % N_2) IN THE MODEL B CRYOPUMP

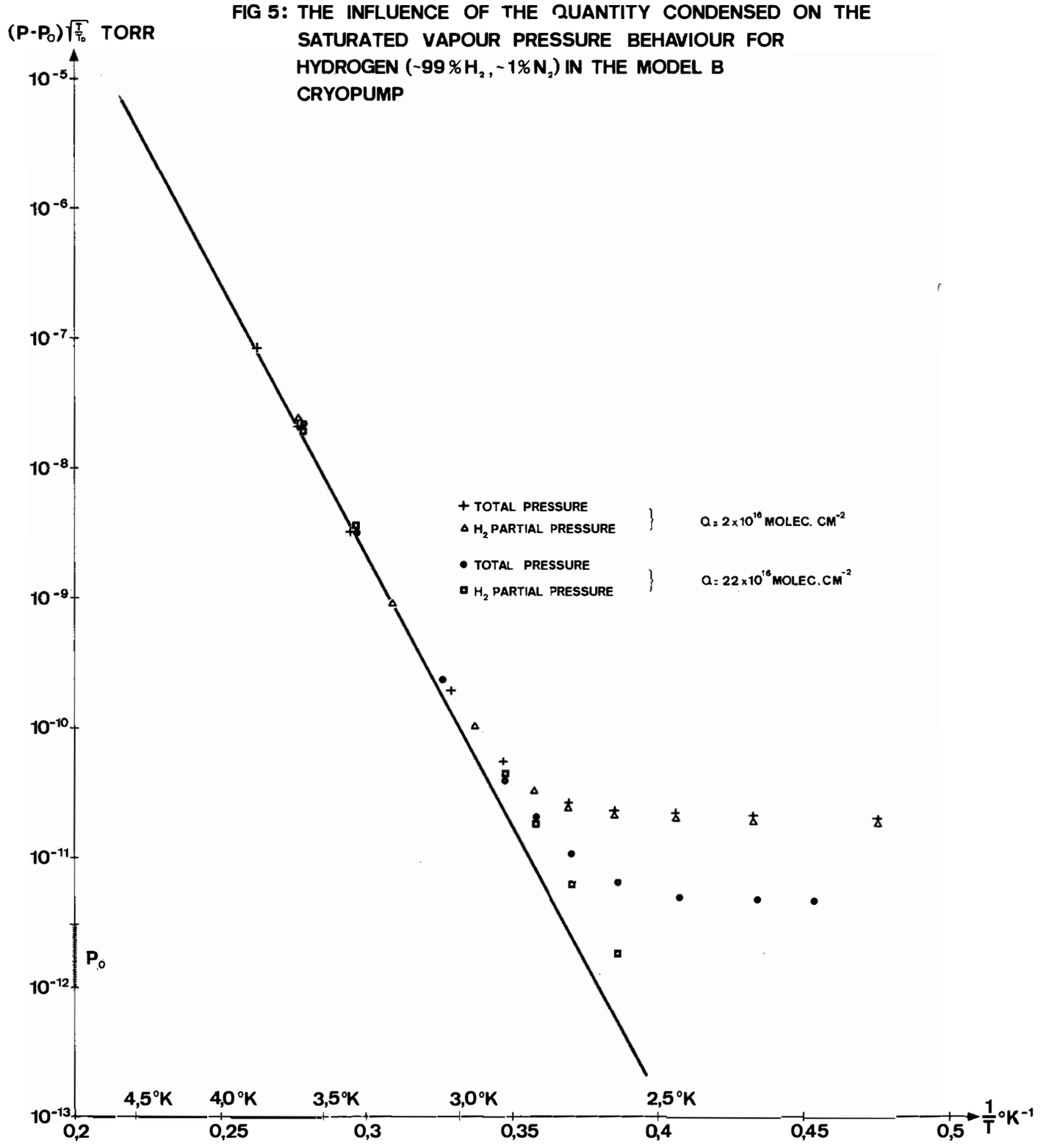

Fig 6 : THE INFLUENCE OF THE HYDROGEN PURITY ON THE EQUILIBRIUM TIMES AND PRESSURES

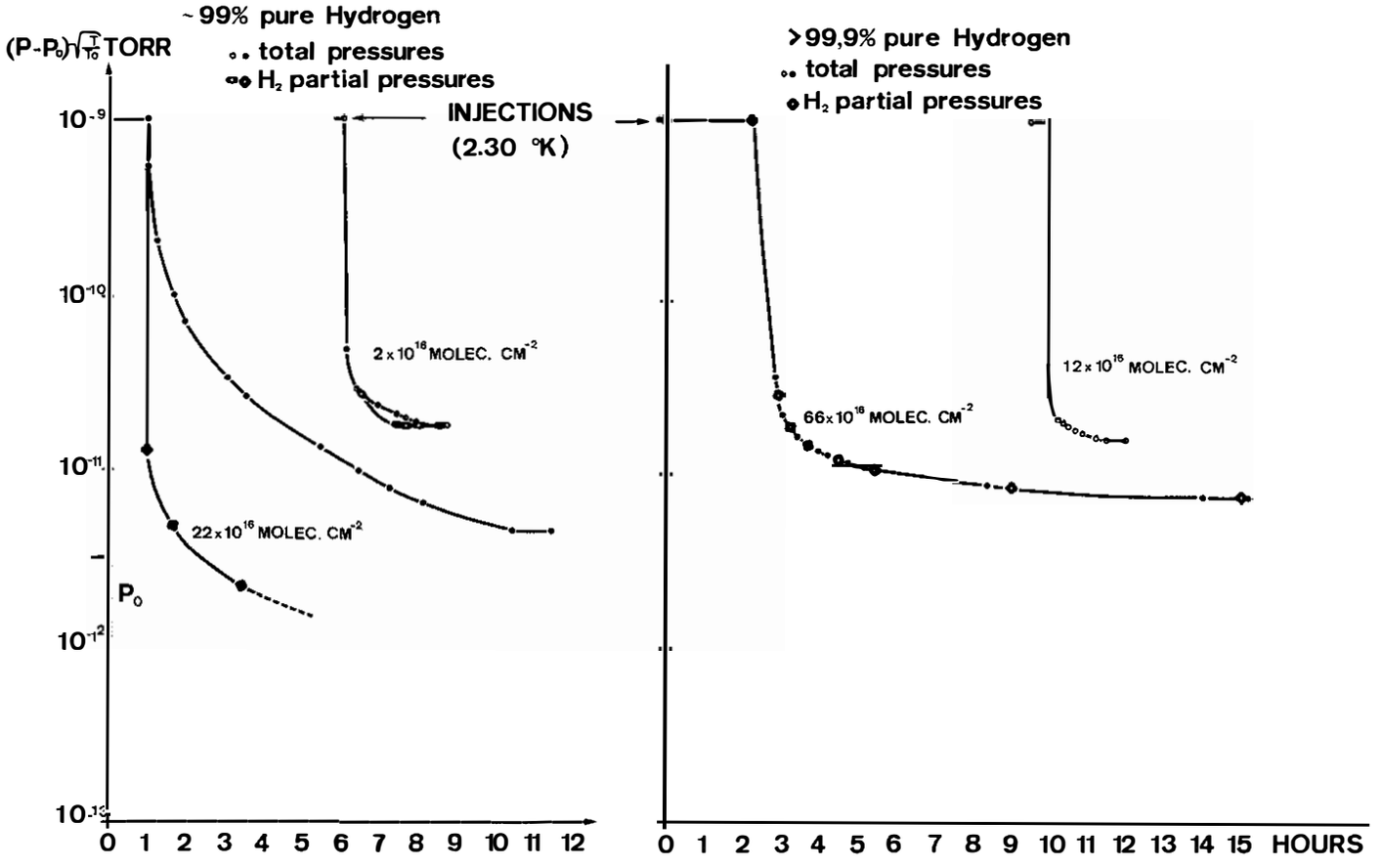

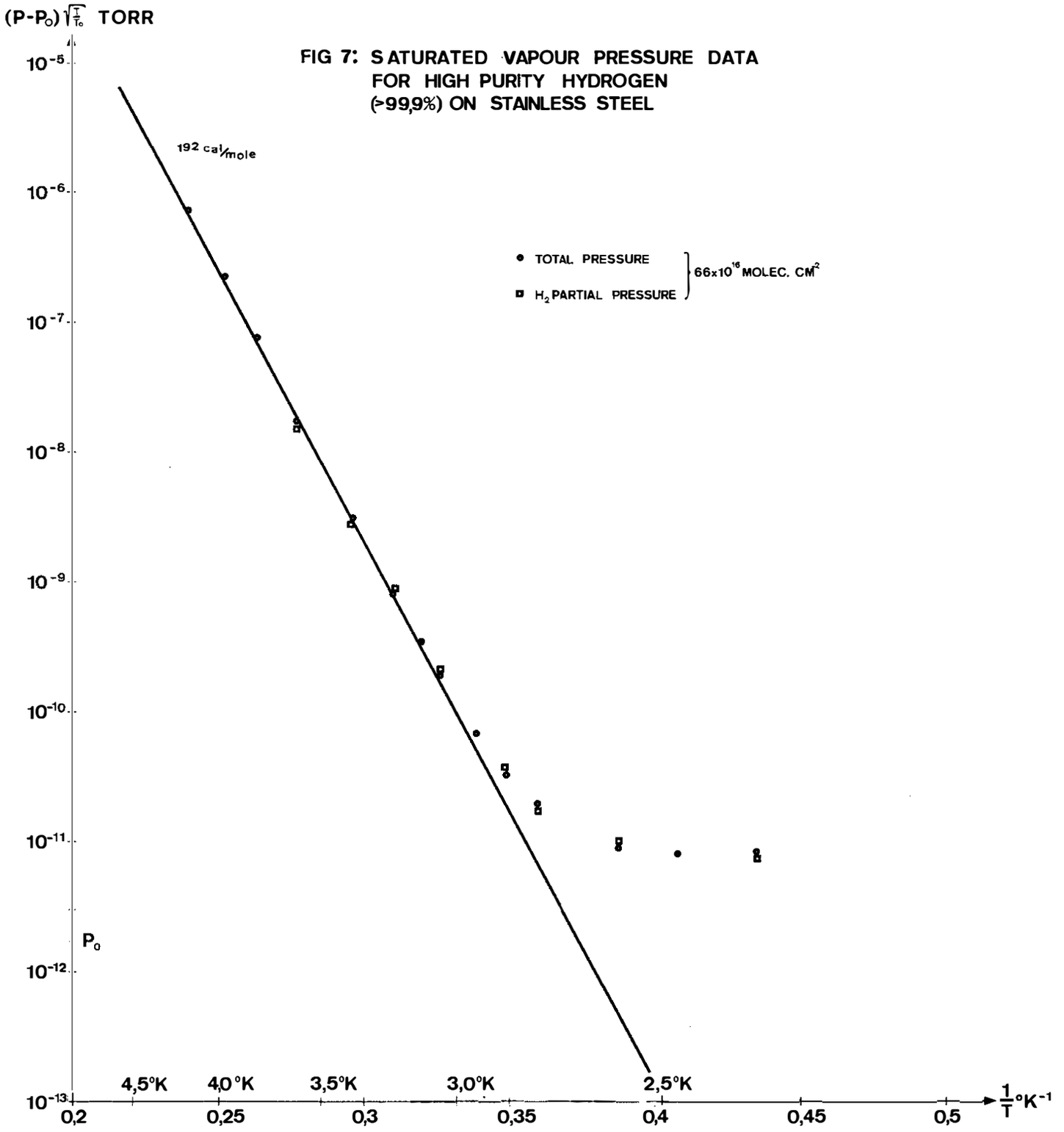

FIG 7: SATURATED VAPOUR PRESSURE DATA FOR HIGH PURITY HYDROGEN (>99,9%) ON STAINLESS STEEL

FIG. 8 : ADSORPTION ISOTHERMS FOR HYDROGEN
OF HIGH PURITY (> 99,9%) ON STAINLESS STEEL

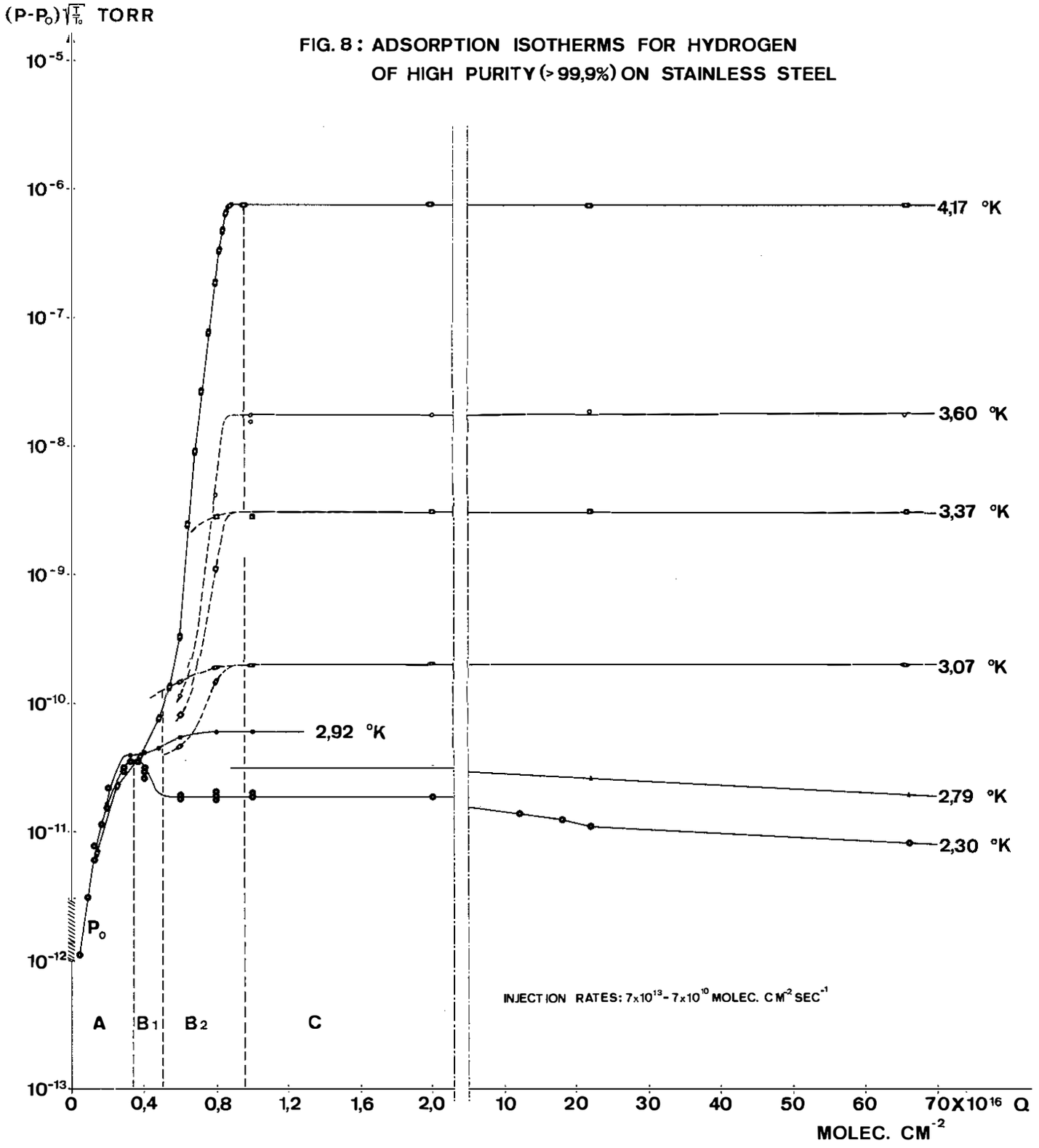

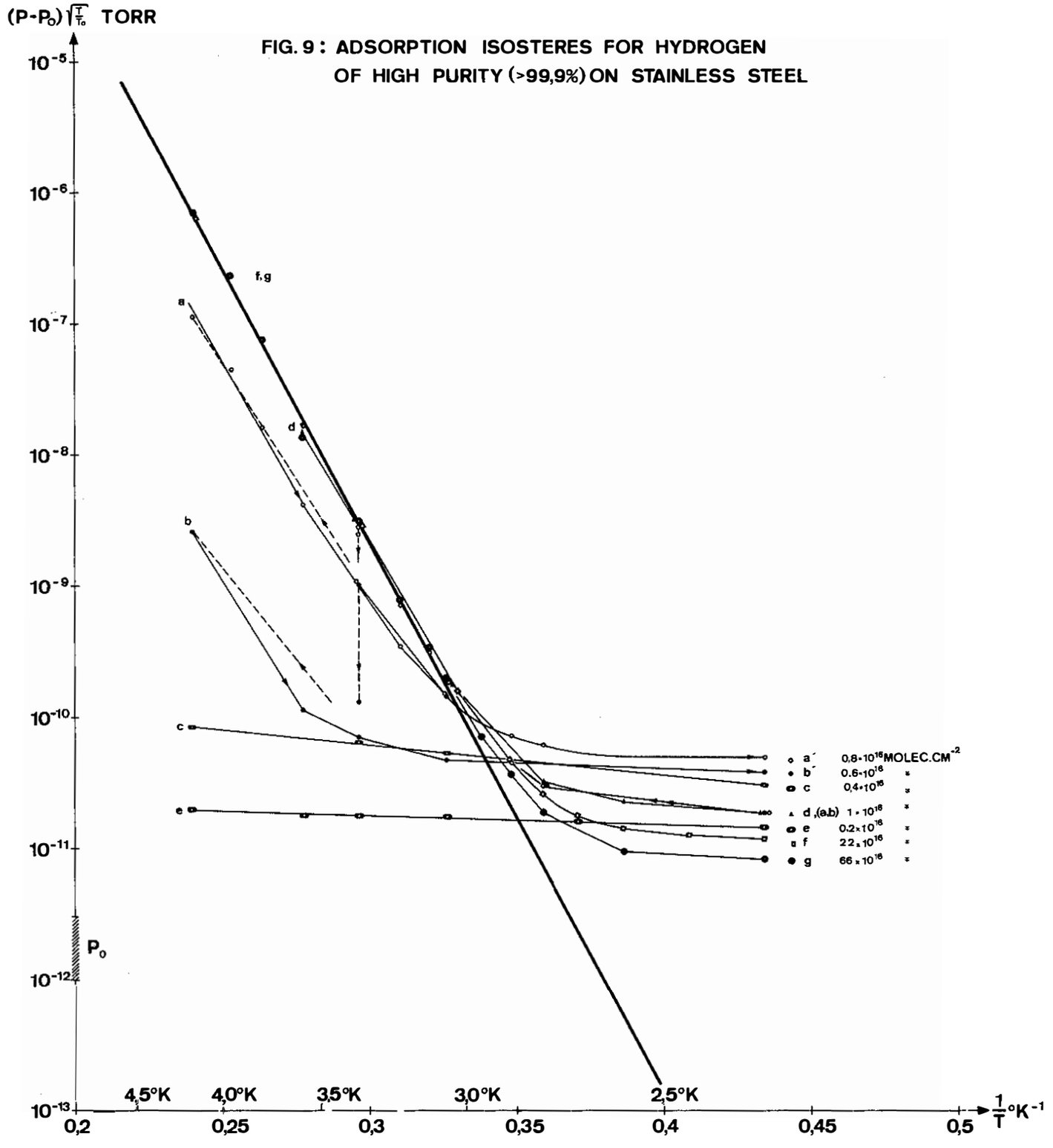
(P-P0)√T/T0 TORR
FIG. 9 : ADSORPTION ISOSTERES FOR HYDROGEN
OF HIGH PURITY (>99,9%) ON STAINLESS STEEL
10-5
10-6
10-7
10-8
10-9
10-10
10-11
10-12
10-13
P0
f,g
a
d
b
c
e
a 0.8·10^15 MOLEC.CM^-2
b 0.6·10^15 "
c 0,4·10^15 "
d ,(a,b) 1·10^15 "
e 0.2·10^15 "
f 2.2·10^15 "
g 66·10^15 "
4,5°K
4,0°K
3,5°K
3,0°K
2,5°K
0,2
0,25
0,3
0,35
0,4
0,45
0,5
1/T °K-1

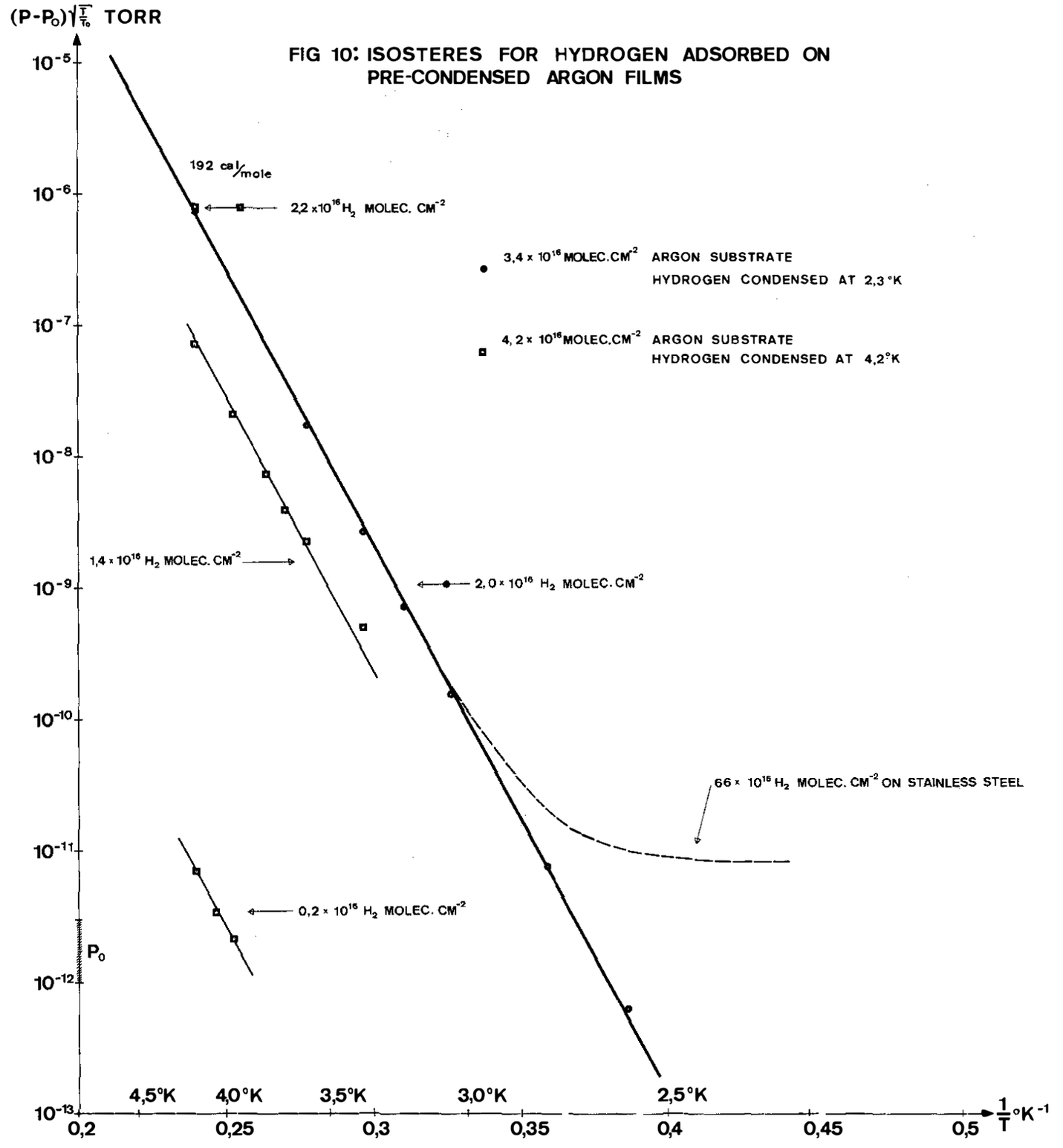
(P-P₀)√(T/T₀) TORR
FIG 10: ISOSTERES FOR HYDROGEN ADSORBED ON PRE-CONDENSED ARGON FILMS
10⁻⁵
10⁻⁶
10⁻⁷
10⁻⁸
10⁻⁹
10⁻¹⁰
10⁻¹¹
10⁻¹²
10⁻¹³
192 cal/mole
2,2 x10¹⁶ H₂ MOLEC. CM⁻²
3,4 x 10¹⁶ MOLEC.CM⁻² ARGON SUBSTRATE
HYDROGEN CONDENSED AT 2,3 °K
4, 2 x 10¹⁶ MOLEC.CM⁻² ARGON SUBSTRATE
HYDROGEN CONDENSED AT 4,2°K
1,4 x 10¹⁶ H₂ MOLEC. CM⁻²
2,0 x 10¹⁶ H₂ MOLEC. CM⁻²
66 x 10¹⁶ H₂ MOLEC. CM⁻² ON STAINLESS STEEL
0,2 x 10¹⁶ H₂ MOLEC. CM⁻²
P₀
4,5°K
4,0°K
3,5°K
3,0°K
2,5°K
0,2
0,25
0,3
0,35
0,4
0,45
0,5
1/T °K⁻¹